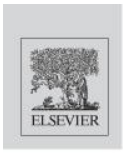
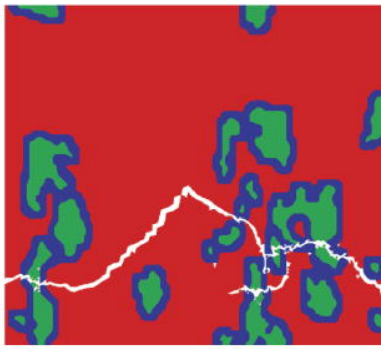
Provided for non-commercial research and education use.
Not for reproduction, distribution or commercial use.



VOLUME 41, issue 1 NOVEMBER 2007
http://www.elsevier.com/locate/commatsci

# COMPUTATIONAL MATERIALS SCIENCE



Editors:
H. DREYSSÉ
S. SCHMAUDER

Available online at
ScienceDirect
www.sciencedirect.com
ISSN 0927-0256

This article was published in an Elsevier journal. The attached copy is furnished to the author for non-commercial research and education use, including for instruction at the author's institution, sharing with colleagues and providing to institution administration.

Other uses, including reproduction and distribution, or selling or licensing copies, or posting to personal, institutional or third party websites are prohibited.

In most cases authors are permitted to post their version of the article (e.g. in Word or Tex form) to their personal website or institutional repository. Authors requiring further information regarding Elsevier's archiving and manuscript policies are encouraged to visit:

http://www.elsevier.com/copyright

Author's personal copy

Available online at www.sciencedirect.com
ScienceDirect
Computational Materials Science 41 (2007) 117–125
COMPUTATIONAL MATERIALS SCIENCE
www.elsevier.com/locate/commatsci

# Prediction of properties of waste AAC aggregate concrete using artificial neural network

İlker Bekir Topçu *, Mustafa Sarıdemir

*Eskişehir Osmangazi University, Department of Civil Engineering, 26480 Eskişehir, Turkey*

Received 13 February 2007; received in revised form 6 March 2007; accepted 12 March 2007
Available online 15 May 2007

**Abstract**

In this study, waste crushed autoclaved aerated concrete aggregates are used as crushed stone in concrete production which have two different sizes in the range of (4–16) and (16–31.5) mm in diameter. Unit weight, cylindrical compressive strength and ultrasound pulse velocity of hardened concrete are determined experimentally for waste autoclaved aerated concrete aggregate concrete types and dynamic elasticity modulus of these concrete types are calculated. It is seen that concrete lighter than crushed stone concrete can be produced by using waste autoclaved aerated concrete aggregates and the usage of waste autoclaved aerated concrete aggregates is suitable for concrete production according to the experimental results. A model is constructed by using artificial neural networks and experimental results are compared to the results of the model. It is concluded that the properties of waste autoclaved aerated concrete aggregated concrete can be obtained without any experimental when the testing in artificial neural networks model results are discussed. It is seen that training and testing results are similar to the experimental results.
© 2007 Elsevier B.V. All rights reserved.

*Keywords:* Autoclaved aerated concrete; Unit weight; Compressive strength; Ultrasound pulse velocity; Artificial neural networks

## 1. Introduction

To recycle waste crushed autoclaved aerated concrete (AAC) in concrete as aggregate is quite important in protecting natural aggregate sources and recycling the waste product that is wanted to be destroyed [1,2]. For these reasons, waste crushed AAC is used in concrete with two different sizes as crushed stone for producing lighter concrete and recycling waste crushed AAC. The effect of the waste crushed AAC aggregates on some hardened concrete properties, like unit weight (UW), compressive strength (CS), ultrasound pulse velocity (UPV) and dynamic modulus of elasticity ($E_d$) values was investigated.

For years, many researchers made good use of various methods for predicting properties of concrete. One of these methods is artificial neural networks (ANN). Yeh [3] applied the ANN for predicting properties of high performance concretes. Lai and Serra [4] predicted the strength of concrete by using the neural network. Lee [5] used single and multiple ANN architecture for predicting of concrete strength. Bai et al. [6] developed neural network models that provide effective predictive capability in respect of the workability of concrete incorporating metakaolin and fly ash. Ji-Zong et al. [7] developed an automatic knowledge-acquisition system based on neural networks to design concrete mix. This system consist of three models: the mix-design model, the slump-prediction model is the core of the system with the other two models supporting the core. Hong-Guang and Ji-Zong [8] proposed a method to predict 28 days compressive strength of concrete by using multi-layer feed-forward neural networks. Dias and Pooliyadda [9] utilized back propagation neural networks to predict the strength and slump of ready mixed concrete and high strength concrete in which chemical admixtures and/or mineral additives were used. Pala et al. [10] developed a model for predicting long-term effects of fly ash

* Corresponding author. Tel.: +90 222 239 3750/3217; fax: +90 222 239 3613.
*E-mail address:* ilkerbt@ogu.edu.tr (İ. Bekir Topçu).

0927-0256/$ - see front matter © 2007 Elsevier B.V. All rights reserved.
doi:10.1016/j.commatsci.2007.03.010

Author's personal copy



and silica fume on compressive strength of concrete by using neural networks. Öztaş et al. [11] constructed a model with two hidden layers for predicting the compressive strength and slump of high strength concrete using neural network. Akkurt et al. [12] used genetic algorithms and ANN for modelling of compressive strength of cement mortar. In the study, the common three-layer feed-forward type of artificial neural networks is used. Mukherjee and Biswas [13] constructed a model with two hidden layers feed-forward type of ANN for predicting the mechanical behavior of concrete at high temperature. Consequently, it is seen that ANN are one of the widespread methods for predicting concrete properties.

In this study, ANN method was also preferred in order to predict the properties of waste crushed AAC aggregated concrete without performing any experiments. The hardened concrete properties used in model of ANN method is the results determined by previous experimental studies. In training of the model; cement (C), water (W), sand (S), crushed stone-I (CS-I), crushed stone-II (CS-II), fine autoclaved aerated concrete (FAAC) and coarse autoclaved aerated concrete (CAAC) were entered as input; while UW, CS, UPV and $E_d$ values were used as output. After training the models without entering the experimental results, tests were performed only with experimental input and values similar to the experimental results were obtained. The network used in ANN method is a multilayer, feed-forward model where backwards distribution of error algorithm is employed [14–16].

## 2. Experimental study

In the experimental study CEM I 42.5 R type cement; granulated sized washed sand from riverbed in the range of 0–4 mm; 5.8 mg/l sulfate contained, 3.9 mg/lt hardness and 6.3 pH tap water; granule sized crushed 4–16 and 16–31.5 mm; and two different groups of 4–16 and 16–31.5 mm granulated sized waste AAC aggregates were used. In waste crushed AAC aggregated concrete, for determining the hardened concrete properties, mixtures were prepared whose crushed stones between the ranges of 4–16 and 16–31.5 mm and replacing crushed stones by using 0%, 50% and 100% waste crushed AAC aggregates. The weights of the materials in 1 $m^3$ concrete mixture were given in Table 1. The mixtures prepared were filled in molds with $\phi 15 \times 30$ cm height. The experiments were carried out at 28 days on samples that had been continuously cured at $20 \pm 2$ °C and $95 \pm 5$ relative humidity. Twenty-eight days later UW, CS and UPV experiments were conducted on the concrete samples produced. $E_d$ values of produced samples were determined regarding ultrasound pulse velocity and unit weight values.

## 3. Results

### 3.1. Unit weight

In the experiments, UW values of the 28 days' concrete series samples that produced with using fine and coarse waste crushed AAC aggregates at 0%, 50% and 100% volume ratios replacing aggregates were determined as given in Fig. 1. Approximately, the UW values of concrete

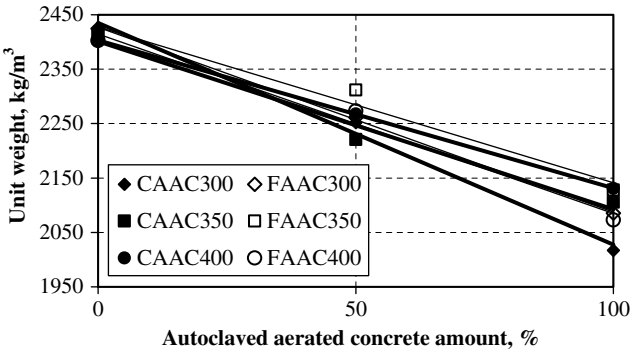



Fig. 1. Variation of UW with AAC amount.

Table 1
1 $m^3$ volume mixture values in waste crushed AAC aggregated concretes

| Mixture, kg | S | CS-I (4–16 mm) | FAAC (4–16 mm) | CS-II (16–31.5 mm) | CAAC (16–31.5 mm) | W | C |
|---|---|---|---|---|---|---|---|
| N300-0 | 739 | 581 | 0 | 581 | 0 | 170 | 300 |
| CAAC300-50 | 739 | 581 | 0 | 291 | 73 | 170 | 300 |
| CAAC300-100 | 739 | 581 | 0 | 0 | 146 | 170 | 300 |
| FAAC300-50 | 739 | 291 | 72 | 581 | 0 | 170 | 300 |
| FAAC300-100 | 739 | 0 | 144 | 581 | 0 | 170 | 300 |
| N350-0 | 721 | 568 | 0 | 568 | 0 | 170 | 350 |
| CAAC350-50 | 721 | 568 | 0 | 284 | 71 | 170 | 350 |
| CAAC350-100 | 721 | 568 | 0 | 0 | 142 | 170 | 350 |
| FAAC350-50 | 721 | 284 | 71 | 568 | 0 | 170 | 350 |
| FAAC350-100 | 721 | 0 | 141 | 568 | 0 | 170 | 350 |
| N400-0 | 705 | 555 | 0 | 555 | 0 | 170 | 400 |
| CAAC400-50 | 705 | 555 | 0 | 278 | 68 | 170 | 400 |
| CAAC400-100 | 705 | 555 | 0 | 0 | 136 | 170 | 400 |
| FAAC400-50 | 705 | 278 | 69 | 555 | 0 | 170 | 400 |
| FAAC400-100 | 705 | 0 | 138 | 555 | 0 | 170 | 400 |

Author's personal copy



samples were observed to vary between 2000 and 2430 kg/m$^3$. The UW values of the concrete decreased by the increase of the waste crushed AAC amount. The decrease in UW value of crushed AAC aggregated produced with CAAC aggregated was greater than produced with FAAC aggregates. The maximum decrease in UW values was 16.82% on an average for 300 dosage 100% CAAC aggregated concrete while the minimum decrease was 4.23% on an average for 350 dosage 50% FAAC aggregated concrete. The decrease in UW values is also evaluated according to average of fine and coarse crushed AAC aggregated concretes at 50% and 100% in all series without caring dosage conditions. In this situation; the maximum decrease was about 14% for 100% CAAC aggregated concretes while the minimum decrease was about 5.5% for 50% FAAC aggregated concretes. The average decreases in UW values in AAC aggregated concretes are shown in Table 2. Experimental results demonstrate that using of crushed waste AAC aggregate in concrete causes a decrease in UW values. This state can be explained with specific gravity of waste AAC aggregates is less than crushed stone's. AAC aggregated concretes' UW regression equations and the multiple regression correlation coefficients are given in Table 3.

### 3.2. Compressive strength

In the experiments, as the amount of AAC increased, CS values of the 28 days' concrete series samples that produced with using fine and coarse waste crushed AAC aggregates at 0%, 50% and 100% volume ratios replacing aggregates were decreased as given in Fig. 2. Approximately, the CS values of concrete samples were observed to vary between 40 and 11 MPa. The maximum decrease in CS values was 68.17% on an average for 350 dosage 100% CAAC aggregated concrete while the minimum decrease was about 31.63% on an average for 300 dosage 50% FAAC aggregated concrete. The decrease in CS values is also evaluated according to average of fine and coarse crushed AAC aggregated concretes at 50% and 100% in all series without caring dosage conditions. In this situation; the maximum decrease was about 66% for 100% CAAC aggregated concretes while the minimum decrease was about 34% for 50% FAAC aggregated concretes. The average decreases in CS values in AAC aggregated concretes are shown in Table 4. The reason of this decrease is that AAC aggregates are forming more

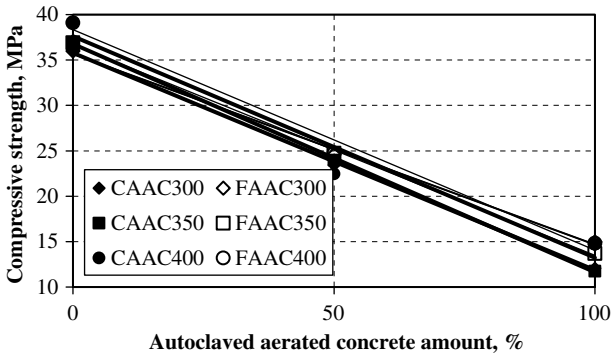



Fig. 2. Variation of CS with AAC amount.

Table 2
The average decrease in UW of AAC aggregated concretes

| Dosage | CAAC, % | | FAAC, % | |
|---|---|---|---|---|
| | 50 | 100 | 50 | 100 |
| 300 | 7.13 | 16.82 | 6.74 | 14.00 |
| 350 | 8.00 | 12.79 | 4.23 | 11.85 |
| 400 | 5.61 | 11.31 | 5.38 | 13.72 |

Table 4
The average decrease in CS of AAC aggregated concretes

| Dosage | CAAC, % | | FAAC, % | |
|---|---|---|---|---|
| | 50 | 100 | 50 | 100 |
| 300 | 34.78 | 66.48 | 31.63 | 58.37 |
| 350 | 35.06 | 68.17 | 33.02 | 62.89 |
| 400 | 42.49 | 62.35 | 36.68 | 62.09 |

Table 3
Regression equations and the $R^2$ values of the AAC aggregated concretes

| Code | Regression equation Unit weight | $R^2$ | Regression equation Compressive strength | $R^2$ |
|---|---|---|---|---|
| CAAC300 | $y = -203.92x + 2639.0$ | 0.9924 | $y = -11.962x + 47.757$ | 0.9993 |
| FAAC300 | $y = -169.69x + 2596.5$ | 0.9995 | $y = -10.508x + 46.196$ | 0.9976 |
| CAAC350 | $y = -154.33x + 2555.2$ | 0.9793 | $y = -12.580x + 49.358$ | 0.9997 |
| FAAC350 | $y = -143.06x + 2570.5$ | 0.9734 | $y = -11.603x + 48.307$ | 0.9992 |
| CAAC400 | $y = -135.84x + 2538.6$ | 0.9987 | $y = -12.193x + 49.804$ | 0.9579 |
| FAAC400 | $y = -164.83x + 2579.2$ | 0.9846 | $y = -12.138x + 50.482$ | 0.9889 |
| | Ultrasound pulse velocity | | Modulus of elasticity | |
| CAAC300 | $y = -0.312x + 5.1156$ | 0.9987 | $y = -10.555x + 67.541$ | 0.9978 |
| FAAC300 | $y = -0.420x + 5.2200$ | 0.9998 | $y = -11.820x + 68.478$ | 0.9970 |
| CAAC350 | $y = -0.380x + 5.1078$ | 0.9328 | $y = -10.790x + 65.474$ | 0.9310 |
| FAAC350 | $y = -0.292x + 5.0567$ | 0.9837 | $y = -9.030x + 65.043$ | 0.9951 |
| CAAC400 | $y = -0.185x + 4.8011$ | 0.8429 | $y = -6.417x + 58.422$ | 0.9494 |
| FAAC400 | $y = -0.423x + 5.0578$ | 0.9350 | $y = -10.928x + 63.221$ | 0.9682 |

Author's personal copy



porosity in concrete and having less strength than crushed stone. Also as can be seen from experimental results; using AAC aggregates in concrete has negative effects on CS. The CS regression equations and the multiple regression correlation coefficients of the AAC aggregated concretes on which experiments were performed are listed on Table 3.

### 3.3. Ultrasound pulse velocity

At the end of 28 days, UPV experiments were conducted on the waste AAC aggregated concrete that were produced for CS experiments. Also as seen in Fig. 3, as the amount of waste crushed AAC increased, UPV values were decreased. The maximum decrease in UPV values was 18.53% on an average for 400 dosage 100% FAAC aggregated concrete while the minimum decrease was 1.02% on an average for 400 dosage 50% CAAC aggregated concrete. The decrease in UPV values is also evaluated according to average of fine and coarse crushed AAC aggregated concretes at 50% and 100% in all series without caring dosage conditions. In this situation; the maximum decrease was about 16% for 100% FAAC aggregated concretes while the minimum decrease was about 6% for 50% CAAC aggregated concretes. The average decreases in UPV values in AAC aggregated concretes are shown in Table 5. The UPV regression equations and the multiple regression correlation coefficients of the AAC aggregated concretes on which experiments were performed are listed on Table 3.

### 3.4. Dynamic modulus of elasticity

Dynamic modulus of elasticity is calculated regarding UW and UPV experimental results of waste crushed AAC aggregated concrete series samples. Also as seen in Fig. 4, as the amount of waste AAC increased, $E_d$ values

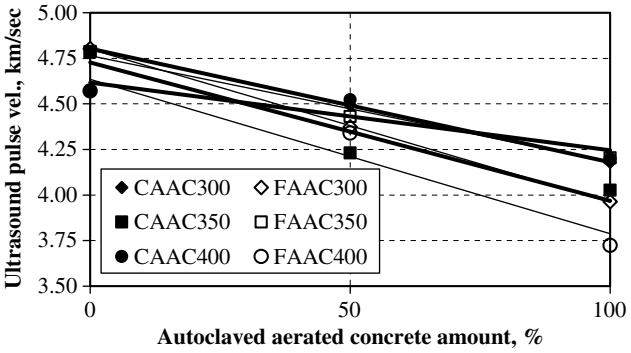



Fig. 3. Variation of UPV with AAC amount.

Table 5
The average decrease in UPV of AAC aggregated concretes

| Dosage | CAAC, % | | FAAC, % | |
|---|---|---|---|---|
| | 50 | 100 | 50 | 100 |
| 300 | 6.45 | 12.97 | 8.95 | 17.49 |
| 350 | 11.63 | 15.88 | 7.45 | 12.18 |
| 400 | 1.02 | 8.10 | 5.03 | 18.53 |

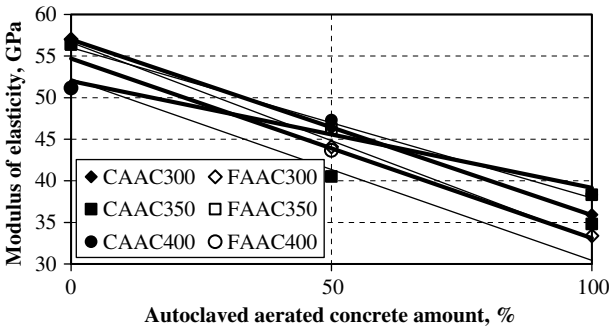



Fig. 4. Variation of $E_d$ with AAC amount.

Table 6
The average decrease in $E_d$ of AAC aggregated concretes

| Dosage | CAAC, % | | FAAC, % | |
|---|---|---|---|---|
| | 50 | 50 | 100 | 100 |
| 300 | 18.72 | 22.67 | 37.00 | 41.44 |
| 350 | 28.15 | 17.87 | 38.28 | 32.02 |
| 400 | 7.53 | 14.66 | 35.09 | 42.73 |

were decreased. The average maximum decrease in $E_d$ values was 42.73% on an average for 400 dosage 100% FAAC aggregated concrete while the minimum decrease was 7.53% on an average for 400 dosage 50% CAAC aggregated concrete. The decrease in $E_d$ values is also evaluated according to average of fine and coarse crushed AAC aggregated concretes at 50% and 100% in all series without caring dosage conditions. In this situation; the maximum decrease was about 39% for 100% FAAC aggregated concretes while the minimum decrease was about 18% for 50% CAAC aggregated concretes. The average decreases in UPV values in AAC aggregated concretes are seen in Table 6. The $E_d$ regression equations and the multiple regression correlation coefficients of the AAC aggregates concretes on which experiments were performed are listed on Table 3.

## 4. Artificial neural network

Artificial neural networks (ANN) are a functional abstraction of the biological neural structures of the central nervous system [16–19]. ANN which can be described as data processing operations may also be perceived as a kind of black box which produces output in respond to the input given. The first studies on ANN are supposed to have started in 1943. McCulloch and Pitts defined artificial neurons for the first time and developed a cell model as in Fig. 5 [12–16]. Afterwards, as a second hit, in 1958 Frank Rosenblatt devised a machine called the perceptron that operated much in the same way as the human mind. A perceptron is a connected network that simulates an associative memory. The most basic perceptron is composed of an input layer and an output layer of nodes, each of which are fully connected to the other. A weight is assigned to each connection which can be adjusted in such a manner when a set of inputs is given to the network, the associated

Author's personal copy



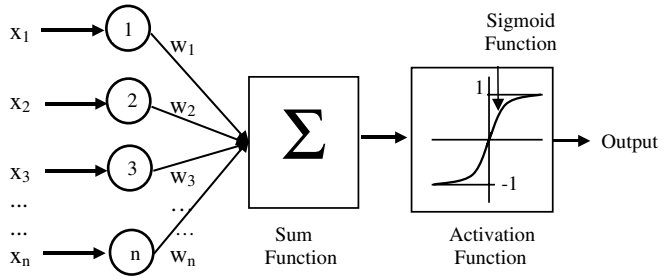



Fig. 5. A simple neuron model.

connections will produce a desired output. Adjusting of these weights to produce a particular output is called "training" of the network which is the mechanism that permits the network to learn. Perceptrons are among the earliest and most basic models of ANN, yet they are in use in many of today's complex neural net applications. As a result of these studies, among the developments in computer technology, use of ANN has become more efficient after 1980 [14,19].

An artificial neuron is composed of five main parts: inputs, weights, sum function, activation function and outputs. Inputs are information that enters the cell from other cells of from external world. Weights are values that express the effect of an input set or another process element in the previous layer on this process element. Sum function is a function that calculates the effect of inputs and weights totally on this process element. This function calculates the net input that comes to a cell [10–19]. The weighted sums of the input components $(\text{net})_j$ are calculated by using Eq. (1) as follows:

$$(\text{net})_j = \sum_{i=1}^{n} w_{ij} x_i + b \tag{1}$$

where $(\text{net})_j$ is the weighted sum of the $j$. neuron for the input received from the preceding layer with $n$ neurons, $w_{ij}$ is the weight between the $j$. neuron in the preceding layer, $x_i$ is the output of the $i$. neuron in the preceding layer [14,20,21]. $b$ a fix value as internal addition and $\sum$ represents sum function. Activation function is a function that processes the net input obtained from sum function and determines the cell output. In general for multi-layer receptive models as the activation function ($f(\cdot)$) sigmoid function is used. The output of the $j$. neuron $(out)_j$ is calculated employing Eq. (2) with a sigmoid function as follows [10–16,21]:

$$(\text{out})_j = f(\text{net})_j = \frac{1}{1 + e^{-\alpha(\text{net})_j}} \tag{2}$$

where $\alpha$ is a constant used to control the slope of the semi-linear region. The sigmoid nonlinearity activates in every layer except in the input layer [20]. The sigmoid function represented by Eq. (2) gives outputs in $(0, 1)$. If it desired, the outputs of this function can be adjusted to $(-1, 1)$ interval. As the sigmoid processor represents a continuous function it is especially used in non-linear descriptions. Because of its derivatives can be determined easily with regard to the parameters within $(\text{net})_j$ variable [10–18].

ANN can supply meaningful answers even when the data to be processed include errors or are incomplete and can process information extremely rapidly when applied to solve engineering problems [14,22,23]. Neuro-computing architectures can be built into physical hardware or neuro-software that can think and act intelligently like human beings. Among various architectures and paradigms, the back-propagation network is one of the simplest and most applicable networks being used in performing higher level of human task such as diagnosis, classification, decision-making, planning and scheduling [24]. The back-propagation is one of the most popular learning algorithms. Accordingly, for a given input pattern, a flow of activation is forwarded from the input layer to the output layer via the hidden layer(s). Then the errors in the output are initiated. The neural network based modeling process determination; (a) data acquisition, analysis and problem representation; (b) architecture determination; (c) learning process determination; (d) training of the networks; and (e) testing of the trained network for generalization evaluation [25].

## 5. Neural network model structure and parameters

In the study 45 experiment results were used in the processes of ANN model. Twenty-three of the experiments were used for the training of the model and 22 were used for testing the trained model. Seven properties; C, S, CS-I, CS-II, FAAC, CAAC and W amounts were used in the input layer and UW, CS, UPV and $E_d$ values of the hardened concrete were used in the output layer. In the ANN model, as seen in Fig. 6, two unit hidden layers were selected. In the first hidden layer 7 and in the second hidden layer 8 cells were determined. The non-linear sigmoid function was used in the hidden layer and the cell outputs at the output layer. Momentum rate and learning rate values were determined and the model was trained through iterations. The trained model was only tested with the input

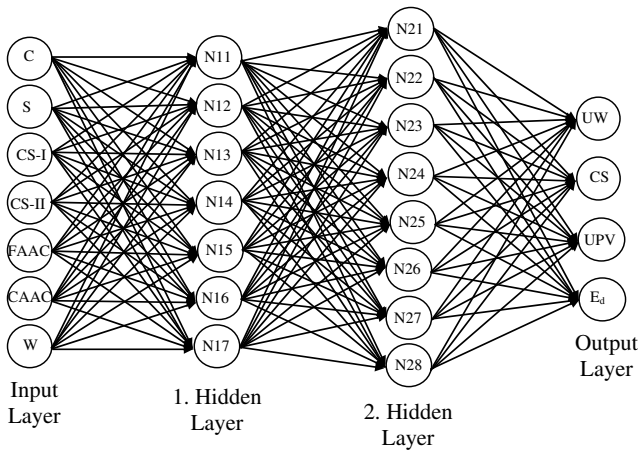



Fig. 6. The system used in the ANN model.

Author's personal copy



values and the results predicted were close to experiment results.

The values of parameters used in this research are as follows:

- Number of input layer units = 7
- Number of hidden layer = 2
- Number of first hidden layer units = 7
- Number of second hidden layer units = 8
- Number of output layer units = 4
- Momentum rate = 0.99
- Learning rate = 0.96
- Error after learning = 0.00016

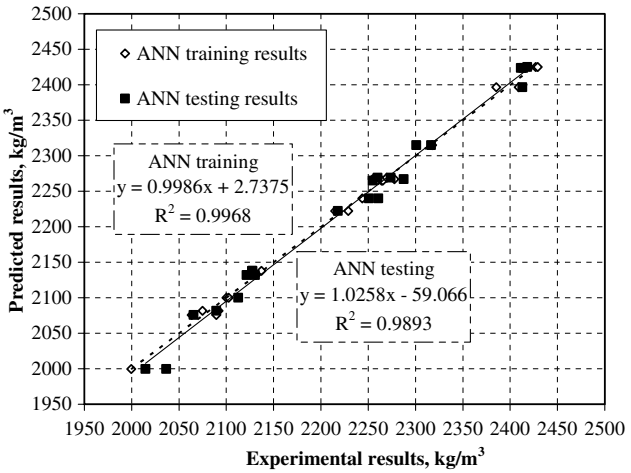



Fig. 7. Comparison of the experimental results of UW with the results of ANN.

### 5.1. Neural network unit weight results

The UW values reached both from the training and testing in ANN model, and from experiments were found as seen in Fig. 7. The linear least square fit line, its equation and the $R^2$ values are shown in these figures for the training and testing data. Also, experimental results and testing results obtained from ANN model were given in Table 7. The absolute error percentage rates of UW values predicted from the training and testing in ANN model is given in Fig. 8. In the training and testing in ANN model the maximum absolute error was determined as 1.81%; the minimum absolute error as 0.00%. Also, the statistical values for UW values found from training and testing in ANN model as a root-mean-squared (RMS) error, absolute fraction of variance ($R^2$) and mean absolute percentage error (MAPE) are also given in Table 8. While the statistical values RMS, $R^2$ and MAPE from training in ANN model were found as 7.3284, 99.98% and 0.2524, respectively, these values were found in testing as 13.5226, 99.97% and

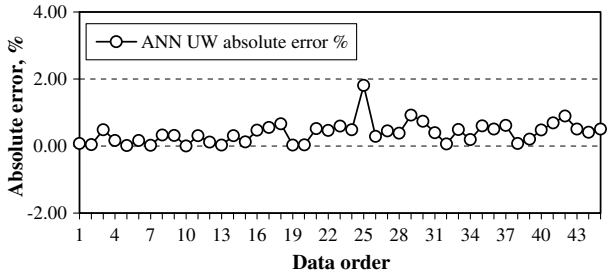



Fig. 8. The absolute error distribution of ANN UW results.

Table 7
Comparison of experimental results with testing results obtained from ANN

| UW | | CS | | UPV | | $E_d$ | |
|---|---|---|---|---|---|---|---|
| Experimental | ANN model | Experimental | ANN model | Experimental | ANN model | Experimental | ANN model |
| 2250.90 | 2239.93 | 23.92 | 22.77 | 4.50 | 4.51 | 46.46 | 46.57 |
| 2036.59 | 1999.80 | 11.99 | 11.81 | 4.15 | 4.22 | 35.75 | 36.15 |
| 2418.19 | 2425.08 | 36.62 | 35.50 | 4.78 | 4.82 | 56.32 | 57.39 |
| 2254.72 | 2264.94 | 24.17 | 24.50 | 4.43 | 4.34 | 45.11 | 43.42 |
| 2089.55 | 2081.58 | 14.66 | 14.79 | 3.95 | 3.97 | 33.23 | 33.31 |
| 2260.76 | 2239.93 | 23.39 | 22.77 | 4.46 | 4.51 | 45.84 | 46.57 |
| 2014.60 | 1999.80 | 12.11 | 11.81 | 4.17 | 4.22 | 35.71 | 36.15 |
| 2413.91 | 2423.51 | 37.06 | 35.79 | 4.77 | 4.82 | 55.99 | 57.35 |
| 2316.49 | 2315.03 | 24.86 | 23.88 | 4.45 | 4.46 | 46.76 | 46.91 |
| 2121.41 | 2131.91 | 13.76 | 13.33 | 4.19 | 4.20 | 37.97 | 38.12 |
| 2217.89 | 2222.06 | 23.71 | 23.77 | 4.25 | 4.22 | 40.84 | 40.13 |
| 2112.75 | 2100.01 | 12.02 | 11.37 | 4.08 | 4.00 | 35.85 | 34.10 |
| 2411.32 | 2423.51 | 37.62 | 35.79 | 4.76 | 4.82 | 55.69 | 57.35 |
| 2300.90 | 2315.03 | 25.16 | 23.88 | 4.38 | 4.46 | 45.00 | 46.91 |
| 2130.35 | 2131.91 | 13.75 | 13.33 | 4.22 | 4.20 | 38.67 | 38.12 |
| 2273.68 | 2269.04 | 23.10 | 22.30 | 4.48 | 4.56 | 46.52 | 48.08 |
| 2127.82 | 2138.00 | 14.52 | 15.17 | 4.17 | 4.22 | 37.72 | 38.68 |
| 2413.05 | 2396.44 | 37.87 | 39.65 | 4.58 | 4.56 | 51.60 | 50.90 |
| 2287.55 | 2267.12 | 25.74 | 24.12 | 4.37 | 4.32 | 44.53 | 43.18 |
| 2065.35 | 2075.73 | 14.74 | 14.79 | 3.77 | 3.70 | 29.92 | 28.92 |
| 2259.8 | 2269.04 | 21.90 | 22.30 | 4.53 | 4.56 | 47.27 | 48.08 |
| 2127.19 | 2138.00 | 14.31 | 15.17 | 4.21 | 4.22 | 38.43 | 38.68 |

Author's personal copy



Table 8
The UW statistical values of proposed ANN model

| Statistical parameters | Unit weight | |
|---|---|---|
| | Training set | Testing set |
| RMS | 7.3284 | 13.5226 |
| $R^2$ | 0.9998 | 0.9997 |
| MAPE | 0.2524 | 0.5315 |

Table 9
The CS statistical values of proposed ANN model

| Statistical parameters | Compressive strength | |
|---|---|---|
| | Training set | Testing set |
| RMS | 0.4093 | 0.9177 |
| $R^2$ | 0.9997 | 0.9984 |
| MAPE | 1.5201 | 3.3271 |

0.5315, respectively. As it is obvious in the error percentage distribution in Fig. 8, the values reached from ANN are very closer to the experimental results.

### 5.2. Neural network compressive strength results

The CS values reached both from the training and testing in ANN model, and from experiments were obtained as seen in Fig. 9. Also, the error percentage rates of CS values reached from training and testing in ANN model is given in Fig. 10. Also, experimental results and testing results obtained from ANN model were given in Table 7. If the CS values reached from the training and testing in ANN according to error rates evaluated; the maximum absolute error was found as 6.28%; the minimum absolute error as 0.01%. Also, the statistical values for CS values found from training and testing in ANN model as RMS, $R^2$ and MAPE are also given in Table 9. While the statistical values RMS, $R^2$ and MAPE from training in ANN model were found as 0.4093, 99.97% and 1.5201, respectively, these values were found in testing as 0.9177, 99.84% and 3.3271, respectively. If the values reached from the training and testing in ANN model is evaluated in terms of error rates, all the values are very closer to the experimental results.

### 5.3. Neural network ultrasound pulse velocity results

The UPV values reached both from the training and testing in ANN model, and from experiments were obtained as shown in Fig. 11. When the experimental results are compared to the results of ANN the values seem to be very similar as Fig. 12. Also, experimental results and testing results obtained from ANN model were given in Table 7. This proves that the experimental results and the ANN results are all in harmony. If the UPV results from

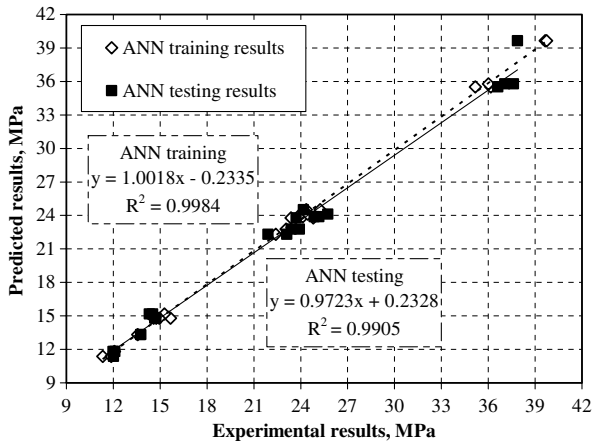



Fig. 9. Comparison of the experimental results of CS with the results of ANN.

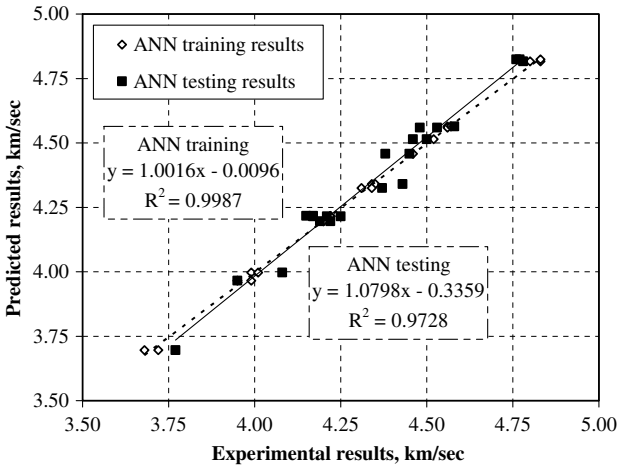



Fig. 11. Comparison of the experimental results of UPV with the results of ANN.

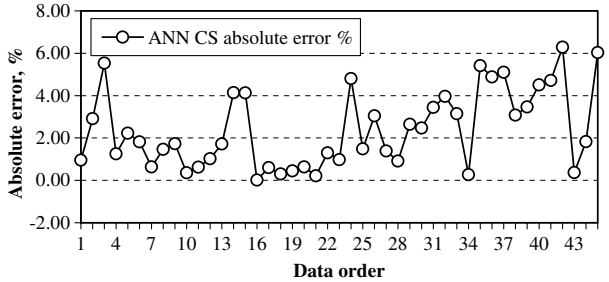



Fig. 10. The absolute error distribution of ANN CS results.

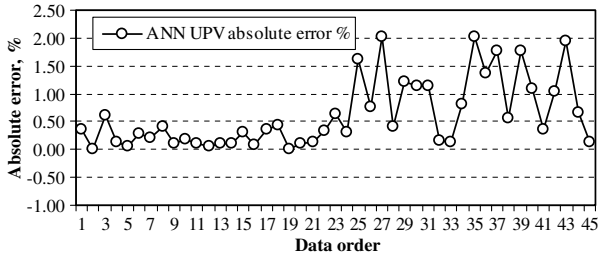



Fig. 12. The absolute error distribution of ANN UPV results.

Author's personal copy



Table 10
The UPV statistical values of proposed ANN model

| Statistical parameters | Ultrasound pulse velocity | |
|---|---|---|
| | Training set | Testing set |
| RMS | 0.0116 | 0.0504 |
| $R^2$ | 0.9999 | 0.9998 |
| MAPE | 0.2238 | 1.0210 |

Table 11
The $E_d$ statistical values of proposed ANN model

| Statistical parameters | Dynamic modulus of elasticity | |
|---|---|---|
| | Training set | Testing set |
| RMS | 0.2609 | 1.0302 |
| $R^2$ | 0.9998 | 0.9994 |
| MAPE | 0.5116 | 2.0180 |

the training and testing in ANN evaluated according to error types; the maximum absolute error was found as 1.98%; the minimum absolute error as 0.01%. Also, the statistical values for UPV values found from training and testing in ANN model as RMS, $R^2$ and MAPE are also given in Table 10. While the statistical values RMS, $R^2$ and MAPE from training in ANN model were found as 0.0116, 99.99% and 0.2238, respectively, these values were found in testing as 0.0504, 99.98% and 1.0210, respectively.

### 5.4. Neural network dynamic modulus of elasticity results

The $E_d$ values reached both from the training and testing in ANN model, and from UW and UPV were calculated as shown in Fig. 13. When calculated $E_d$ results are compared to the results of ANN, the values are similar to each other as seen in Fig. 14. Also, experimental results and testing results obtained from ANN model were given in Table 7. This proves that the calculated $E_d$ results and the ANN results are all in harmony. If the $E_d$ results from the training and testing in ANN was evaluated according to error types; the maximum absolute error was found as 4.88%; the minimum absolute error as 0.06%. Also, the statistical values for $E_d$ values found from training and testing in ANN model as RMS, $R^2$ and MAPE are also given in Table 11. While the statistical values RMS, $R^2$ and MAPE from training in ANN model were found as 0.2609, 99.98% and 0.5116, respectively, these values were found in testing as 1.0302, 99.94% and 2.0180, respectively.

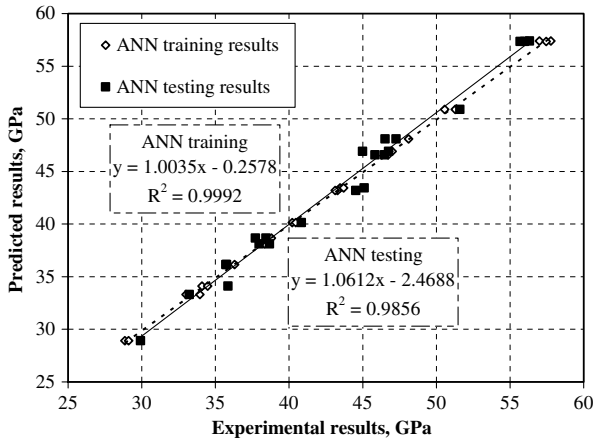



Fig. 13. Comparison of calculated the $E_d$ values with the results of ANN.

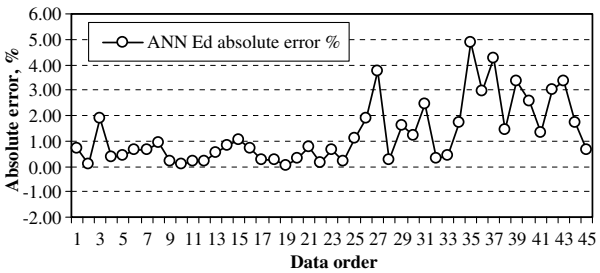



Fig. 14. The absolute error distribution of ANN $E_d$ values.

## 6. Conclusions

- As the amount of waste crushed autoclaved aerated concrete aggregates used in concrete replacing crushed stone has increased, the hardened unit weight values have decreased. Unit weight values decreasing is greater in coarse crushed autoclaved aerated concrete aggregated concretes compared to the fine crushed autoclaved aerated concrete aggregated ones.
- As a result of the increase in the amount of waste crushed autoclaved aerated concrete aggregated concrete used replacing crushed stone, the compressive strength of waste crushed autoclaved aerated concrete aggregated concrete has excessively decreased.
- Ultrasound pulse velocity, which is another property of hardened concrete, has decreased as the amount of the waste autoclaved aerated concrete aggregates used replacing crushed stone increased.
- The dynamic modulus of elasticity values calculated from UW and UPV has decreased as the amount of the waste crushed autoclaved aerated concrete aggregates used replacing crushed stone increased.
- In order to predict the unit weight, cylinder compressive strength, ultrasound pulse velocity and dynamic modulus of elasticity values of the waste crushed autoclaved aerated concrete aggregated hardened concretes without attempting any experiments model was constructed in ANN method. The model was trained with input and output data. In trained model using only the input data; unit weight, cylinder compressive strength, ultrasound pulse velocity and dynamic modulus of elasticity values of hardened concrete were predicted. The obtained values are very closer to the experimental results. As a result, it was shown that, unit weight, compressive strength, ultrasound pulse velocity and dynamic modulus of elasticity values of the waste crushed autoclaved aerated concrete aggregated concretes can be predicted in ANN model in a quite short period of time with tiny error rates.

Author's personal copy



## References


[1] İ.B. Topçu, M. Canbaz, Cement and Concrete Research 34 (2) (2004) 267–274.
[2] İ.B. Topçu, A. Demir, C. Karakurt, The usage of autoclaved aerated concrete in concrete as aggregate, in: Kocaeli Earthquake Symposium, 2005, pp. 857–863.
[3] I.C. Yeh, Cement and Concrete Research 28 (12) (1998) 1797–1808.
[4] S. Lai, M. Sera, Construction and Building Materials 11 (2) (1997) 93–98.
[5] S–C. Lee, Engineering Structures 25 (2003) 849–857.
[6] J. Bai, S. Wild, J.A. Ware, B.B. Sabir, Advances in Engineering Software 25 (2003) 663–669.
[7] W. Ji-Zong, N. Hong-Guang, H. Jin-Jun, Cement and Concrete Research 29 (1999) 1875–1880.
[8] N. Hong-Guang, W. Ji-Zong, Cement and Concrete Research 30 (2000) 1245–1250.
[9] W.P.S. Dias, S.P. Pooliyadda, Construction and Building Materials 15 (2001) 371–379.
[10] M. Pala, E. Özbay, A. Öztaş, M.I. Yuce, Construction and Building Materials 21 (2) (2007) 384–394.
[11] A. Öztaş, M. Pala, E. Özbay, E. Kanca, N. Çağlar, M. Asghar Bhatti, Construction and Building Materials 20 (9) (2006) 769–775.
[12] S. Akkurt, S. Ozdemir, G. Tayfur, B. Akyol, Cement and Concrete Research 33 (7) (2003) 973–979.
[13] A. Mukherjee, S.N. Biswas, Nuclear Engineering and Design 178 (1997) 1–11.
[14] İ.B. Topçu, M. Sarıdemir, Prediction of rubberized concrete properties using artificial neural network and fuzzy logic, Construction and Building Materials, in press.
[15] J.J. Hopfield, Proceedings of the National Academy of Sciences 79 (1982) 2554–2558.
[16] J.A. Anderson, Cognitive and psychological computation with neural models, IEEE Transactions on Systems, Man and Cybernetics 5 (1983) 799–814, V.SMC-13.
[17] H.M. Gunaydın, S.Z. Dogan, International Journal of Project Manage 22 (7) (2004) 595–602.
[18] M.A. Arbib, The Handbook of Brain Theory and Neural Networks, MIT Press, Cambridge (MA), 1995.
[19] J.A. Anderson, An introduction to computing with neural nets, A Bradford book, MIT Press, Cambridge (MA), 1995.
[20] S.W. Liu, J.H. Huang, J.C. Sung, C.C. Lee, Computer Methods in Applied Mechanics Engineering 191 (2002) 2831–2845.
[21] A.T. Seyhan, G. Tayfur, M. Karakurt, M. Tanoğlu, Computational Materials Science 34 (2005) 99–105.
[22] R.P. Lippman, An introduction to computing with neural nets, in: Artificial Neural Networks. The computer society theoretical concepts. Washington, 1988, pp. 36–54.
[23] M.Y. Rafing, G. Bugmann, D.J. Easterbrook, Computer Structure 79 (2001) 1541–1552.
[24] B. Sohabhon, O.O. Spethen, Engineering Construct Architect Manage 6 (2) (1999) 133–144.
[25] X. Wu, S.Y. Lim, in: Prediction maximum scour depth at the spur dikes with adaptive neural networks, Neural Networks and Combinatorial Optimization in Civil and Structural Engineering, Civil-Comp Press, Edinburgh, 1993, pp. 61–66.